Information Fusion 18 (2014) 1–8

Contents lists available at ScienceDirect

Information Fusion

journal homepage: www.elsevier.com/locate/inffus

Using multi-sensor data fusion for vibration fault diagnosis of rolling element bearings by accelerometer and load cell

M.S. Safizadeh *, S.K. Latifi

School of Mechanical Engineering, Iran University of Science and Technology, Tehran, Iran

ARTICLE INFO

Article history:
Received 22 February 2012
Received in revised form 11 October 2013
Accepted 11 October 2013
Available online 28 October 2013

Keywords:
Bearing diagnosis
Pattern recognition
Multiple sensor fusion
Accelerometer
Load cell

ABSTRACT

This paper presents a new method for bearing fault diagnosis using the fusion of two primary sensors: an accelerometer and a load cell. A novel condition-based monitoring (CBM) system consisting of six modules: sensing, signal processing, feature extraction, classification, high-level fusion and decision making module has been proposed. To obtain acceleration and load signals, a work bench has been used. In the next stage, signal indices for each signal in both time and frequency domains have been calculated. After calculation of signal indices, principal component analysis is employed for redundancy reduction. Two principal features have been extracted from load and acceleration indices. In the fourth module, K-Nearest Neighbor (KNN) classifier has been used in order to identify the condition of the ball bearing based on vibration signal and load signal. In the fifth module, a high-level sensor fusion is used to derive information that would not be available from single sensor. Based on situation assessment carried out during the training process of classifier, a relationship between bearing condition and sensor performance has been found. Finally, a logical program has been used to decide about the condition of the ball bearing. The test results demonstrate that the load cell is powerful to detect the healthy ball bearings from the defected ones, and the accelerometer is useful to detect the location of fault. Experimental results show the effectiveness of this method.

1. Introduction

Bearing is a key element in rotating machinery and any defect can cause malfunctioning of machine. Normally, defects initiate and grow during bearing operation. Detection of defects at an early stage is of great importance because it can prevent the progression of defects to other parts of machine. Condition-based monitoring (CBM) procedure is established to improve quality inspection, and predictive maintenance. So far, a variety of methods are used for the diagnosis of bearing defects. The methods are broadly classified as acoustic measurements [1], current and temperature monitoring [2], wear debris detection [3], and vibration analysis [4]. Acoustic Emission (AE) is considered as the most effective acoustic-based bearing health monitoring technique. It is a high frequency, transient impulse emitted by the rapid local stress redistributions in solid material under working load condition. Examples of AE application are crack growth, corrosion and wear. The measurement of transient sound waves in a machine element such as bearing and analysis of acoustic signal properties can be used to detect and localize defects. Al-Ghamd and Mba [5] reported several studies on the application of AE to bearing diagnosis and compared the AE method with vibration based method. Although in compare to other techniques, this technique is considered when structural integrity monitoring is required but its accuracy is limited by the number of used sensors.

Current monitoring for bearing fault detection is relatively new method. It has become an attractive technique for condition monitoring of induction motor ball bearings. This method is simple and available in many applications but the major drawback of this method is the presence of noise and the difficulty of separating bearing faults from non mechanical faults. Another approach is using infrared thermography for detection of bearing degradation. A bearing failure can cause excessive heat generation in the rotating components. Bearing fault detection based on thermography has some limitations such as expensive equipment and hard to detect fault at an early stage. A review of infrared thermography for condition monitoring [6] discussed in details various applications.

Wear debris detection sensor is also used for damage detection in rotating machinery such as gearbox and bearing. The most common oil debris sensors can detect abnormal wear in gearboxes. A disadvantage of this technique is that it does not localize the failure in complicated gearboxes.

Vibration measurement and analysis is widely considered as the most effective condition diagnosis method for rotating

* Corresponding author. Tel.: +98 21 77240540; fax: +98 21 77240488.
E-mail addresses: Safizadeh@iust.ac.ir (M.S. Safizadeh), kourosh_latifi@hotmail.com (S.K. Latifi).

1566-2535/$ - see front matter © 2013 Elsevier B.V. All rights reserved.
http://dx.doi.org/10.1016/j.inffus.2013.10.002

machinery. A local fault in a machine such as spalling on balls/rollers or cracked race in a bearing generates a shock impulse every time the local fault contacts another part of the machine. Thus, the vibrations produced by shock impulses can be analyzed to identify the machine fault. The main advantage of vibration based machine diagnosis is the ability to detect different types of defects, either distributed or localized. Furthermore, low-cost sensors, accurate results, simple setups, specific information on the damage location, and comparable rates of damage are other benefits of the vibration measurement method.

Even a fault-free bearing generates vibration; thus, studying the base-line behavior of bearing oscillation is necessary to find the abnormality in the damaged vibration signature. The principal source of vibration in roller element bearings is varying compliance, caused by the continuous change of position and the number of load carrying elements. Based on this phenomenon, different models have been proposed to represent the periodic vibration of bearings [7,8]. The periodic vibration of bearings can be transformed to chaotic through a quasi-periodic, period doubling, and intermittency routes [4]. Recently, some studies have even shown a possible relation between chaotic parameters and bearing faults. For example, it has been shown that the correlation integral of bearing vibration data [9,10], and the modified Poincare map of vibration data [11] are potential features for fault diagnosis.

The majority of the research on the diagnosis and prognosis of bearings is based on signal processing techniques, independent of bearing vibration characteristics. In these works, first a localized or distributed defect is created on a bearing by means of grinding, acid etching, drilling, overloading, or over speeding to intentionally introduce defects in the bearing components. An accelerometer is usually used to measure vibration signal of the defective bearing. The bearing vibration signal is then analyzed by different signal processing techniques to extract the fault sensitive features that will later be used as the monitoring indices. This procedure is quite similar among the published literature. The reported signal processing methods are categorized as time domain, frequency domain, and time–frequency domain. These techniques are not totally independent, and in many cases, they are complementary to each other. Time domain analysis has been widely employed. Successful results of Root Mean Square (RMS), Kurtosis, skewness, peak value, crest factor (CF), and synchronous averaging [12] have been reported in the low frequency range of less than 5 kHz. Band pass filtering has also been conducted in the time domain. It is based on the fact that the strike between the damage and the rotating component can excite high frequency resonances (10–100 kHz). The generated energy from this impact is not sufficient to excite the entire rotor's assembly, but is enough to excite vibration sensor resonance. Monitoring the vibration amplitude at the resonant band pass filtered frequency is the principle of the shock pulse method [13]. It is implemented in shock pulse meters which are the most accepted diagnostic instrument in the industry.

Time domain analysis has the advantage of simple calculations, straightforward signal pre-processing, and speed independency. However, insensitivity to early stage faults and deeply distributed defects are drawbacks of this approach. Perhaps, frequency domain, also called spectral analysis, is the most reported signal processing method for bearing diagnosis. Each bearing component has a characteristic frequency, which is calculated from the kinematics of the rotating parts. Monitoring these frequencies or their harmonics at a low frequency range (<5 kHz) has been successful in bearing diagnosis [14]; however, some research draws attention to the weakness of this method for detecting small defects [15]. To decrease the effect of the noise level and frequency side bands, some researchers have adopted the amplitude demodulated or enveloped signal. The spectral analysis of a low and/or high frequency range enveloped signal is repeatedly reported as an efficient method for bearing diagnosis. A number of frequency domain features, based on simple or complex signal processing methods such as power cepstrum [12], adaptive noise cancellation [16], and denoising [17], are also proposed for bearing diagnosis. The frequency domain approach is sensitive and robust to detect bearing defects and to identify the localized damage location. However, the accuracy of this method highly depends on the bearing dimensions and rotational speed. In addition, frequency domain methods give good results if the frequency band is carefully selected.

Time–frequency methods can provide useful information regarding energy distribution of a signal in time and frequency domain. In signal processing, a number of time–frequency analysis methods such as the short time Fourier transform, Wigner–Ville distribution, and wavelet transforms [18] have been proposed. Due to its flexibility and computational benefits, wavelet transform is widely used for bearing diagnosis and prognosis [19]. Some researchers have suggested the use of diagnostic features, obtained from wavelet decompositions [20], and wavelet packets [21].

In many cases, particularly in speed and load variable systems, a simple inspection of the monitoring index does not provide reliable information regarding the condition of the machine. Therefore, there is still a demand for reliable, flexible, and automated procedures for the diagnosis of such systems. Artificial Neural Networks (ANNs) with their flexibility and learning capabilities are the best candidates for a decision-making engine of a diagnostic scheme. The input to such a scheme is monitoring indices obtained from signal processing, and the output corresponds to the level of the bearing's health. Different kinds of ANNs are proposed for bearing condition monitoring with time and/or frequency domain features. The multi-layer feed-forward [22], radial basis function [23], wavelet neural networks [24], adaptive resonance theory network, and Adaptive Neuro-Fuzzy Inference System (ANFIS) [25] are among the most referenced networks in bearing condition monitoring. Also, other types of intelligent systems such as pattern recognition models [26], cascade correlation algorithms [27], automated fuzzy inference [28], support vector machine [29], and genetic algorithms [30] have also been employed, to extract the condition of the bearing. Bearing prognosis refers to the adoption of current and previous monitoring indices to forecast machine's future states. Bearing prognostic methods are either model-based life perdition, or intelligent systems. The first category focuses on a model to predict the fatigue life of a bearing, whereas the second category involves statistical or intelligent systems to estimates the future state of a bearing. A few prognostic methods are recently proposed based on Recurrent Neural Network (RNNs) [31], Multi Layer Perception (MLP) [32], and self organizing map [33] with limited applications.

However, the above researches only used the vibration measurements from individual sensors. Integrating the diagnostic tools with different measurement technologies into one system can potentially improve the detection capabilities and probability that damage is detected.

The objective of this research is to combine load and vibration based fault detection techniques using decision fusion in order to obtain a bearing monitoring system with greater efficiency in detection and decision making capabilities than the individual diagnostic tools. The experimental load and vibration measurements will be used to verify this hypothesis.

2. Experimental set-up and measurements

2.1. Test rig

The test rig used in this study is illustrated in Fig. 1. It consists of a single-phase induction motor driving the V-belt drive. The V-belt

Fig. 1. Bearing test rig.

is used to transmit the power through pulley drive. The pulley drive is installed on a shaft which is supported by two ball bearings. One of two bearings is used in order to simulate faulty conditions. Their type is SKF 6307 and similar faults are created by spark erosion technique. A loading system is also used to load the bearing through V-belt drive. In order to isolate the test rig from environmental noise and vibration some rubber sheets were mounted under the test setup supporting legs. The accelerometer and load cell transducers have been mounted on the housing of test bearing.

2.2. Instrumentations

Vibration measurements were carried out by a piezoelectric accelerometer IMI Sensors 608A111 having undamped natural frequency of 10 kHz. The accelerometer's output was sent to the NI-USB-9233 analog to digital which connected to PC. Load was also measured with a miniature load cell SEWHACNM SM601. The output of the load cell was first amplified by a DACELL DN-AM100 amplifier and then sent to NI-USB-9233 analog to digital. The schematic diagram of the measurement block is shown in Fig. 2.

2.3. Measurement conditions

All vibration and load signals were measured under three different speeds of shaft bearing (1000 rpm, 1200 rpm and 1600 rpm) and three loading conditions (the minimum load, the average load and the maximum load). First, a healthy bearing were used for healthy conditions and 9 different conditions were gained by changing V-belt tension load and shaft speed.

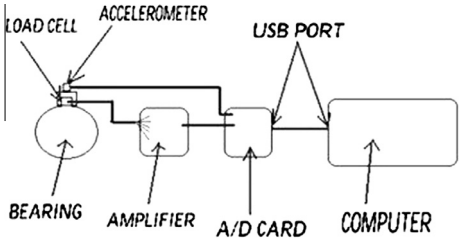

Fig. 2. Schematic diagram of the measurement block.

Failure progression tests were conducted in the test rig. Bearing defects were created on the outer race and ball elements by spark erosion technique. Outer race defect was a crack which its depth varies in three steps of 0.2 mm, 0.4 mm and 0.6 mm. 27 conditions were gained by changing crack depth, crack angle and shaft speed.

Ball defects were also simulated with the same defect sizes as the defects on the outer race (see Fig. 3). 10 conditions were gained by changing crack depth, V-belt tension and shaft speed.

3. Automated condition-based monitoring system

Fig. 4 shows the flow chart of the proposed method for multi-sensor data fusion. This automated condition-based monitoring system consists of six basic modules which are introduced below.

3.1. Data acquisition and signal processing

First, vibration and load data was collected from accelerometer and load cell located on the test bearing housing in radial direction. The signals were recorded for 6 s and ran through an anti-aliasing filter in data acquisition card with sampling frequency of 10 kHz. Time domain signals of healthy and defective bearings are shown in Figs. 5 and 6.

In the next module, the input data is acceleration and load signals and the output is statistical parameters and signal indices. In this research, signal analysis was carried out in both time and frequency domains which are introduced below.

3.1.1. Time domain analysis

Time domain analysis, due to its simplicity, has always been an attractive approach for bearing diagnosis. The simplest method is to measure the overall RMS level of the bearing vibration. However, this technique is not sensitive to small or early-stage defects. The crest factor is the ratio of the peak acceleration to the RMS value. Ingarashi et al. [34] have reported that the level of the crest factor for a normal bearing is approximately five. These authors have proven that the crest factor is a good indicator of small size defects; although, when localized damage propagates, the value of the crest factor decreases significantly due to the increasing RMS. The vibration peak level can also be employed as a monitoring index; but is found to be unreliable for small size defects.

The Kurtosis, the fourth normalized statistical moment, corresponds to the peakedness of the data. For an undamaged bearing, this amount is equal to three in the low frequency bands. Many researchers have found the Kurtosis value to be more useful, when it is compared with the RMS, crest factor, and peak value.

In this research, 10 parameters were obtained from each signal in time domain. Kurtosis, crest factor, K factor, Variance, Peak level, Standard deviation, RMS, Skewness, Mean and Median of the signal were contributed in this approach.

3.1.2. Frequency domain analysis

For bearing fault diagnosis, frequency domain, or spectral analysis, is the most popular approach. Many researchers have reported successful results for detecting damaged bearings through spectral analysis. Usually, it is carried out at low-range frequencies and the defects are identified by the change of the spectral amplitude at each of the characteristic frequencies. Taylor [14] has formulated the sequence of appearing and disappearing spikes in the spectrum. In addition, he has proposed a method for measuring the size of the defects on the raceways.

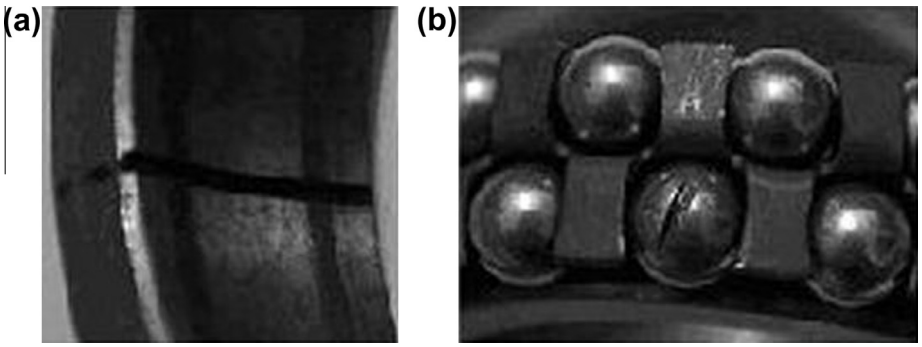

Fig. 3. Double-row self-aligning ball bearing damaged by electric current (a) outer race fault and (b) ball fault.

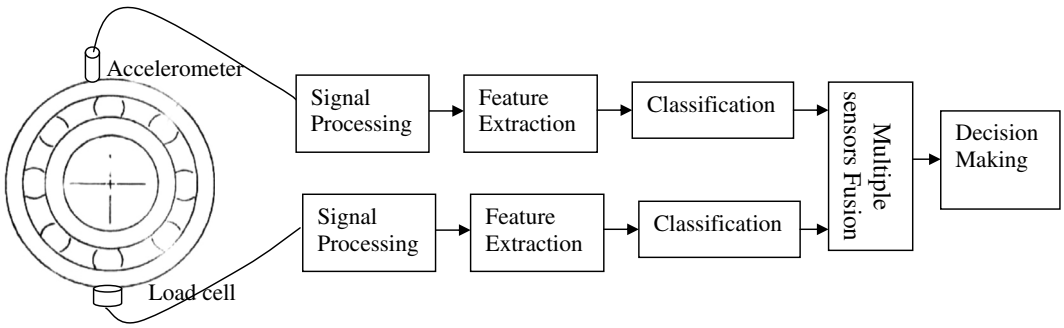

Fig. 4. Flow chart of the proposed fusion method.

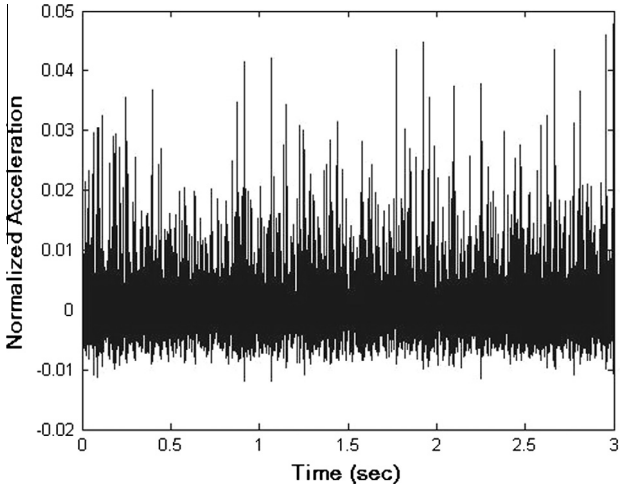

Fig. 5. Time acceleration signal of a healthy bearing condition.

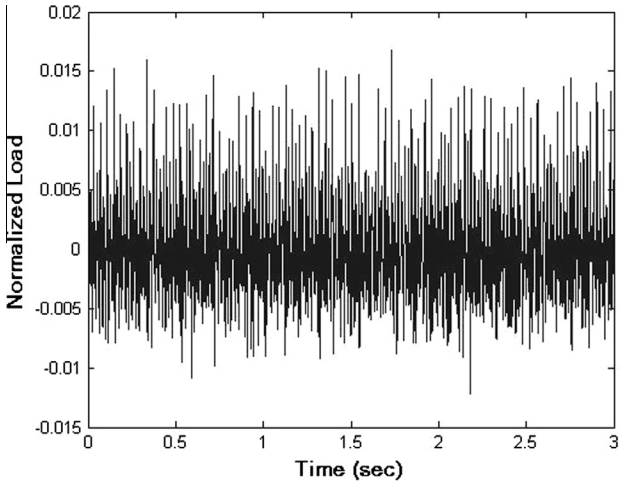

Fig. 6. Time load signal measured by a load cell on a bearing with outer race defect.

The envelope detection is a well-defined technique for bearing fault diagnosis. The efficiency of this method has been evaluated and can also be combined with an auto detection filter band and spectrum analyzer. Ho and Randal [16] have conducted extensive research on the envelope technique. Their work has demonstrated that a Self-Adaptive Noise Cancellation (SANC) method, in conjunction with an envelope analysis improves a bearing's diagnostic results.

In this research, two parameters were obtained from each signal in frequency domain. These parameters were included amplitude in ball pass frequency of outer race and ball spin frequency which are obtained according to theoretical dynamic relations. Features matrix of acceleration is shown in Table 1. Features matrix of load is shown in Table 2.

3.2. Features extraction

Diagnosis is most commonly performed as classification using feature-based techniques. The features extraction module is implemented for the process of mapping the original measurements (features) into fewer features without losing any important information. At this stage, the time and frequency features are calculated for the load and vibration sensor.

In this study, Principal Components Analysis (PCA) was used to feature reduction module. PCA provides a subset of information containing the most important information and reduces dimensionality by eliminating data redundancy. Such unsupervised data compression has a wide range of applications such as meteorology, image processing, genomic analysis, and information retrieval.

Table 1
Features matrix of acceleration.

Class	Name	Variance	Kurtosis	Mean	Std	Skew	Peak	Median	RMS	Crest	K factor	Out FR A	Ball FR A
1	F1-S3	0.112	12.7639	0.0012	0.1057	1.8342	0.7739	−0.0081	0.1057	7.3228	0.0818	3.0435	4.9302
1	F1-S2	0.0043	15.2688	6.57E−04	0.0658	2.1457	0.5583	−0.0067	0.0658	8.4802	0.0368	2.7542	4.5362
1	F1-S1	0.0017	16.1299	0.001	0.0413	1.6547	0.4286	−0.0014	0.0414	10.3639	0.0177	2.8003	4.837
1	F2-S3	0.0225	13.2028	0.0011	0.1501	2.456	0.9377	−0.0268	0.1501	6.248	0.1407	3.2138	5.1648
1	F2-S2	0.0045	17.2516	0.001	0.0668	2.2267	0.6173	−0.0055	0.0668	9.2442	0.0412	2.0962	4.0937
1	F2-S1	0.0119	12.3548	0.0012	0.1091	1.8121	0.7124	−0.0053	0.1091	6.5319	0.0777	2.9237	4.1536
1	F3-S3	0.0326	14.8988	0.0012	0.1805	2.5902	1.2858	−0.0388	0.1805	7.1232	0.2321	2.8917	5.4389
1	F3-S2	0.0104	11.0889	0.001	0.1018	1.9602	0.668	−0.0124	0.1018	6.5628	0.068	3.1527	4.2091
2	S3-0.3-D0	0.0095	19.7636	0.0012	0.0975	2.3059	0.7817	−0.0026	0.0975	8.0158	0.0762	3.8492	5.6473
2	S3-0.3-D90	0.0241	25.1227	0.0012	0.1551	3.4245	1.194	−0.0121	0.1551	7.6968	0.1852	4.962	5.5574
2	S3-0.3-D180	0.0438	13.5738	0.0011	0.2093	2.5386	1.2666	0.0343	0.2093	6.0523	0.2651	3.2673	5.0493
2	S3-0.3-D0	0.0041	28.2769	0.0012	0.0639	2.5857	0.6835	−0.0023	0.0639	10.6975	0.0437	3.5491	5.9309
2	S2-0.3-D90	0.0477	17.9845	0.0011	0.2185	2.9797	1.7614	−0.0326	0.2185	8.062	0.3849	3.739	4.9307
2	S2-0.3-D180	0.0477	17.9845	0.0011	0.2185	2.9797	1.7614	−0.0326	0.2185	8.062	0.3849	2.9371	5.3938
2	S1-0.3-D0	0.0049	23.9709	0.0012	0.07	2.5683	0.657	−0.002	0.07	9.3836	0.046	3.5267	5.9912
2	S1-0.3-D90	0.0108	29.7909	0.0012	0.1039	3.3459	0.9851	−0.0047	0.1039	9.4825	0.1023	4.0064	4.9017
2	S-0.3-D180	0.027	16.9466	0.0011	0.1642	2.7376	1.2212	−0.0161	0.1642	7.4378	0.2005	2.893	5.3946
2	S3-0.6-D0	0.0191	16.5669	0.0011	0.1382	2.6287	1.0105	−0.0172	0.1382	7.3121	0.1397	4.1205	5.3721
2	S3-0.6-D90	0.0234	13.0895	0.0011	0.1531	2.3166	1.0261	−0.0236	0.1531	6.7004	0.1571	5.2038	4.4503
2	S3-0.6-D180	0.1059	16.277	0.0011	0.3254	2.8512	2.0298	−0.0514	0.3254	6.2388	0.6604	3.5647	5.9382
2	S2-0.6-D0	0.0397	17.6448	0.0011	0.1992	2.9259	1.2778	−0.0255	0.1992	6.4139	0.2546	3.6471	5.0492
2	S2-0.6-D90	0.0087	13.0839	0.0011	0.0932	1.9565	0.8639	−0.008	0.0932	9.269	0.0805	4.4836	5.9362
2	S2-0.6-D180	0.0395	14.5973	0.0011	0.1987	2.6148	1.3622	−0.0269	0.1987	6.8562	0.2707	3.5749	6.9301
2	S1-2.6-D0	0.0043	21.476	0.0011	0.0659	2.4267	0.709	−0.0041	0.0659	10.7583	0.0467	4.2039	6.3902
2	S1-0.6-D90	0.0107	18.8434	0.0012	0.1034	2.6468	0.8566	−0.0106	0.1034	8.2802	0.0886	5.904	5.8457
2	S1-0.6-D180	0.034	15.0917	0.0012	0.1843	2.6764	1.2198	−0.0255	0.1843	6.6173	0.2248	3.9487	5.489
2	S3-0.8-D90	0.0098	10.7345	9.30E−04	0.0988	1.6925	0.6694	−0.0104	0.0998	6.7763	0.0661	4.4356	6.3522
2	S3-0.B-D90	0.1396	20.1365	0.001	0.3736	3.4306	2.643	−0.0684	0.3736	7.0734	0.9875	5.593	5.4901
2	S3-0.8-D180	0.1187	11.1398	0.001	0.3445	2.5253	1.817	−0.1182	0.3445	5.2736	0.626	3.6479	4.9301
2	S2-O.8-D0	0.0042	4.0604	0.0012	0.0647	0.5371	0.3597	−0.0028	0.0647	5.5619	0.0233	4.1998	5.3099
2	S2-0.8-D90	0.0396	14.0758	0.001	0.199	2.5839	1.2927	−0.0458	0.199	6.4971	0.2572	4.8901	5.2911
2	S2-0.8-D180	0.1106	11.0194	0.0011	0.3326	2.479	1.7593	−0.1101	0.3326	5.2895	0.5852	4.9721	6.3092
3	F1-S3-0.3	0.1381	31.2079	0.0011	0.3716	4.1787	3.2444	−0.0684	0.3716	8.7318	1.2055	3.192	7.9348
3	F1-S2-0.3	0.3142	29.5407	6.88E−04	0.5605	4.2507	3.5855	−0.0865	0.5605	6.3964	2.0098	3.2819	7.5654
3	F1-S1-0.3	0.1559	35.6146	0.0011	0.3948	4.4619	3.3984	−0.058	0.3948	8.608	1.3416	2.9028	7.1033
3	F2-S2-0.3	0.1218	31.3883	0.0011	0.349	4.1523	3.0191	−0.0609	0.349	8.6504	1.0537	2.8736	8.2993
3	F1-S3-0.6	0.0606	23.6325	0.001	0.2462	3.4227	2.3652	−0.0526	0.2462	9.6082	0.5822	3.3345	7.2903
3	F1-S2-0.6	0.0235	22.9154	0.0011	0.1532	3.1523	1.4928	−0.0184	0.1532	9.7459	0.2287	3.2903	10.829
3	F1-S1-0.6	0.0223	37.2659	0.0011	0.1492	4.0298	1.6062	−0.0141	0.1492	10.7637	0.2397	3.0009	8.2943
3	F2-S1-0.6	0.1166	26.7509	0.0011	0.3414	3.7239	3.307	−0.049	0.3414	9.6864	1.129	3.9203	7.9586
3	F1-S3-0.8	0.123	25.9351	0.0011	0.3507	3.9847	2.492	−0.0665	0.3507	7.1062	0.8739	3.0377	9.4657
3	F1-S2-0.8	0.0557	29.7472	0.0011	0.2361	4.1335	1.93	−0.0402	0.2361	3.1755	0.4556	3.2993	7.4601

Basically, the dimension reduction of PCA method come from the selection of the dimensions which variances are maximized. Mathematically, this is equivalent to finding the dominant eigenvectors of the scaled. The statistical parameters and signal indices are the input of this module while the 1st and the 2nd principal components are the outputs.

3.3. Classification

Many automatic diagnosis system for rotating machinery use a signal classification in order to increase accuracy and avoid human error identification. In this paper, K-Nearest-Neighbor (KNN) has been applied to ball bearing fault classification. KNN is a simple algorithm that works based on a similarity measure (minimum distance). The KNN process includes two phases: the training and the test phases. The training is the determination of the nearest neighbors and the test is the determination of the class using those neighbors. The KNN finds the nearest neighbors of an observation using the standard Euclidean distance. According to its K nearest neighbors and the distances, an observation is classified. The distance of every test point is calculated from the nearest training point in the principal components plane through Eq. (1).

$$d = \sqrt{(x_1(test) - x_1(train))^2 + (x_2(test) - x_2(train))^2} \quad (1)$$

where x_1 and x_2 denote the first and second principal components of the training and test points; applying Eq. (1), classification borders are obtained for each sensor which is shown in Figs. 7 and 8.

3.4. Multiple sensors fusion

Multiple sensor fusion is a process of combining information collected by different sensors. Multiple sensors fusion can be carried out at three levels: data level, feature level and decision level.

- Data-level fusion

All raw data measured by a number of sensors from an object are combined directly to produce more informative data than the original data. Then, the feature extraction is performed on the fused data following by a pattern recognition process for classification. The fused data at this level is more accurate and reliable than the data achieved from single sensor. However, the data fusion in this level is carried out on the data collected from the sensors which are measuring the same physical quantities or phenomena. As a consequence, the application of data-level fusion is limited to the data from commensurate sensors.

- Feature-level fusion

At this level, the features extracted using signal processing techniques from different sensors are merged together. Feature-le-

Table 2
Features matrix of load.

Class	Name	Variance	Kurtosis	Mean	Std	Skew	Peak	Median	RMS	Crest	K factor
1	F1-S3	4.22E−04	2.6623	0.0013	0.0205	−0.2018	0.0644	0.0018	0.0206	3.1307	0.0013
1	F1-S2	5.60E−04	2.5743	0.0013	0.0237	0.2683	0.0847	4.64E−05	0.0237	3.5746	0.002
1	F1-S1	1.83E−04	2.6234	0.0011	0.0135	−0.0425	0.0492	0.0013	0.0136	3.627	6.68E−04
1	F2-S3	4.32E−04	2.6325	0.0014	0.0208	−0.2094	0.071	0.0021	0.0208	3.4079	0.0015
1	F2-S2	477E−04	2.6521	0.0013	0.0218	−0.0267	0.0697	0.0017	0.0219	3.1881	0.0015
1	F2-S1	4.81E−04	2.4546	−2.82E−04	0.0219	−0.0744	0.1056	−2.18E−04	0.0219	4.8137	0.0023
1	F3-S3	4.44E−04	2.6062	0.0014	0.0211	−0.1911	0.0693	0.0022	0.0211	3.2812	0.0015
1	F3-S2	3.32E−04	2.6312	0.0014	0.0182	0.1859	0.0632	5.14E−04	0.0183	3.4613	0.0012
2	S3-0.3-D0	9.09E−04	3.9985	0.0013	0.0302	0.2136	0.0989	−3.72E−04	0.0302	3.2767	0.003
2	S3-0.3-D90	4.33E−04	3.9523	8.61E−04	0.0208	0.0349	0.0746	9.59E−04	0.0208	3.5825	0.0016
2	S3-0.3-D180	7.73E−04	3.8756	0.0013	0.0278	0.7243	0.1037	−0.0018	0.0278	3.7238	0.0029
2	S2-0.3-D0	4.02E−04	3.8413	0.0013	0.0201	0.1627	0.0648	1.85E−04	0.0201	3.2262	0.0013
2	S2-0.3-D90	4.38E−04	3.7342	0.0012	0.0209	−0.2524	0.0764	0.0024	0.021	3.6456	0.0016
2	S2-0.3-D180	0.0011	3.7248	0.0014	0.0334	0.2598	0.1119	8.44E−05	0.0334	3.3502	0.0037
2	S1-0.3-D0	5.79E−04	3.9414	0.0012	0.0241	0.2208	0.0802	1.86E−04	0.0241	3.331	0.0019
2	S1-0.3-D90	3.99E−04	3.8348	0.0014	0.02	−0.2817	0.0675	0.0028	0.02	3.3691	0.0014
2	S1-0.3-D180	5.61E−04	3.9543	0.0014	0.0237	0.3495	0.0872	−3.46E−04	0.0237	3.6758	0.0021
2	S3-0.6-D0	7.14E−04	3.9007	0.0015	0.0267	0.0983	0.0875	0.0013	0.0268	3.2693	0.0023
2	S3-06-D90	7.18E−04	3.9546	0.0011	0.0268	−0.166	0.0935	0.0022	0.0268	3.4847	0.0025
2	S3-0.6-D180	0.0041	3.8567	0.0014	0.0641	0.0765	0.1608	−0.0014	0.0641	2.5073	0.0103
2	S2-0.6-D0	0.0018	3.9065	0.0014	0.0421	0.0315	0.1223	0.0013	0.0421	2.9068	0.0051
2	S2-0.6-D90	5.32E−04	3.7716	0.0014	0.0231	−0.1678	0.0992	0.0018	0.0231	4.2943	0.0023
2	S2-06-D180	0.0021	3.7198	0.0014	0.0461	−0.2219	0.1376	0.0057	0.0461	2.9836	0.0063
2	S1-0.6-D0	4.49E−04	3.9713	0.0013	0.0212	0.1189	0.0663	4.78E−04	0.0212	3.124	0.0014
2	S1-0.6-D90	5.39E−04	3.8476	0.0014	0.0232	−0.1664	0.0867	0.0024	0.0233	3.7243	0.002
2	S1-0.6-D180	0.0023	3.7184	0.0013	0.0483	−0.0078	0.1516	0.0011	0.0483	3.1388	0.0073
2	S3-0.8-D0	7.63E−04	3.7464	0.001	0.0276	−0.831	0.1262	0.004	0.0276	4.5655	0.0035
2	S3-0.8-D90	0.0122	3.9712	0.0013	0.1103	0.1218	0.266	−0.0039	0.1103	2.4109	0.0293
2	S3-0.8-D180	0.0036	3.8147	0.0011	0.0602	−0.1728	0.2204	0.0036	0.0602	3.66	0.0133
2	S2-0.8-D0	2.94E−04	3.667	0.0015	0.0171	−0.422	0.0675	0.0026	0.0172	3.9218	0.0012
2	S2-0.8-D90	0.0033	3.9648	0.0013	0.0575	−0.0244	0.1829	0.0011	0.0575	3.1796	0.0105
2	S2-0.8-D180	0.0023	3.952	0.0015	0.0484	0.1403	0.1868	−9.33E−04	0.0484	3.8607	0.009
3	F1-S3-0.3	0.004	3.5396	0.0013	0.0635	0.2893	0.2075	−9.41E−04	0.0635	3.2679	0.0132
3	F1-S2-0.3	0.016	3.6501	0.0016	0.1265	0.1141	0.3951	−0.0037	0.1266	3.122	0.05
3	F1-S1-0.3	0.0065	3.7753	0.0015	0.0806	0.1758	0.279	−0.0011	0.0806	3.46	0.0225
3	F2-S2-0.3	0.0041	3.6085	0.0016	0.0642	−0.0864	0.233	0.0016	0.0642	3.6292	0.015
3	F1-S3-0.6	0.0022	3.8762	0.0015	0.0466	−0.1736	0.1622	0.0022	0.0466	3.4805	0.0076
3	F1-S2-0.6	0.0022	3.7501	0.0014	0.0472	0.0148	0.1635	0.0015	0.0472	3.4621	0.0077
3	F1-S1-0.6	0.0014	3.7134	0.0014	0.0375	−0.1254	0.1558	0.0024	0.0375	4.1523	0.0058
3	F2-S1-0.6	0.0055	3.6591	0.0014	0.0744	−0.1402	0.2314	0.0052	0.0744	3.109	0.0172
3	F1-S30.8	0.0034	3.8166	0.0014	0.0579	−0.3855	0.2146	0.0041	0.0579	3.7056	0.0124
3	F1-S2-0.8	0.0028	3.7889	0.0014	0.0529	0.0058	0.1909	7.41E−04	0.0529	3.6076	0.0101

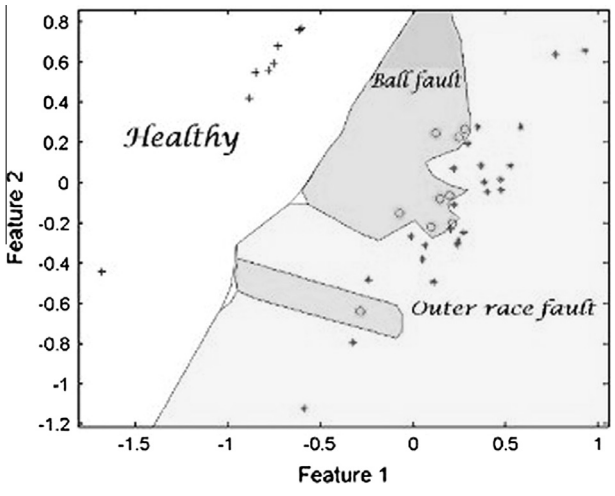

Fig. 7. Illustration of class borders for KNN classification on load cell data.

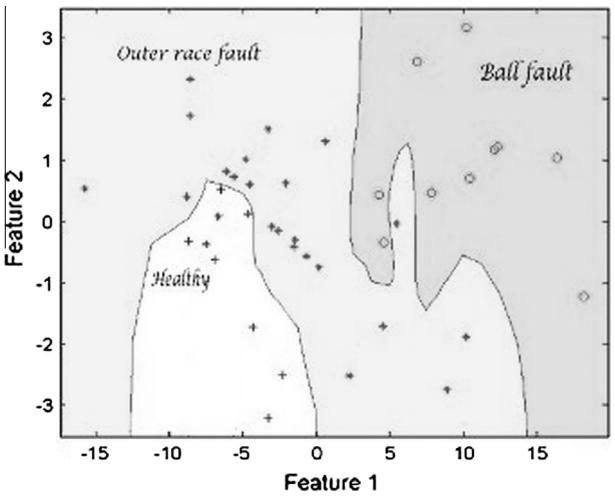

Fig. 8. Illustration of class borders for KNN classification on accelerometer data.

vel fusion is an intermediate level of fusion that involves combining non-commensurate sensors features. All features are fused to find an optimal subset of features which are then fed to a classifier or decision-level fusion.

- Decision-level fusion

Decision-level fusion is a high level of fusion which involves fusion of the results obtained from different sensors. It emphasizes the importance of classifier combination to provide a better result.

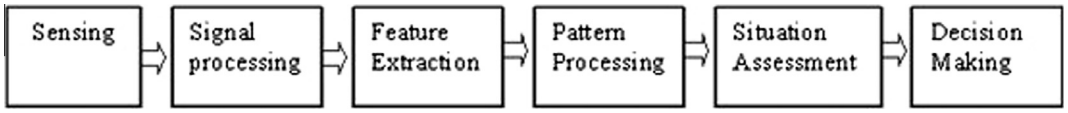

Fig. 9. The Waterfall Fusion Process Model.

Table 3
Effectiveness of each technique.

Bearing condition	Accelerometer detection	Load cell detection	Data fusion technique
Healthy	Outer race fault	Healthy	Healthy
Outer race fault	Outer race fault	Outer race fault	Outer race fault
Outer race fault	Outer race fault	Outer race fault	Outer race fault
Outer race fault	Outer race fault	Outer race fault	Outer race fault
Ball fault	Ball fault	Outer race fault	Ball fault
Ball fault	Ball fault	Outer race fault	Ball fault

The fusion of decisions can also reduce the misclassification rates in terms of both false positives and false negatives.

Since the selection of the above described models depends on the sensor fusion application, there is not a general-purpose model for sensor data fusion. In this study, we focus on an architecture which has been known as Waterfall Fusion Process Model. The waterfall model was proposed in 1997 under the guidance of Great Britain department of defense.

Fig. 9 depicts the process flowchart of the waterfall model. The process steps are as follows: sensing and signal processing correspond to source preprocessing, feature extraction and pattern processing match object refinement, situation assessment or situation refinement, and decision making corresponds to threat refinement.

While the waterfall model is more accurate in analyzing the fusion process than other models, the major drawback of this model is the omission of any feedback data flow.

3.5. Decision making

Nearest-neighbor methods are used for classifying observations. To classify a new observation, its neighborhood is calculated and the probability of membership in each class is determined as relative frequency in the neighborhood. Finally, the class with the highest probability is chosen. Nearest-neighbor models do not need a probabilistic distribution, the fitted values in these models are determined by the training sets, not by explicit rules. The nearest-neighbor models are also called memory-based learning models, as they do not need to fit any model or to estimate any global function. Instead they should store all training observations in memory, and when a classification is required; they recall all training data from memory. Two key players in nearest neighbor-methods are the distance function and the cardinality k of the neighborhood. The distance function is used for measuring the distance between data points; greater distances indicate greater dissimilarities. The most common distance function is Euclidean distance; however it can also be Manhattan, Mahalanobis, Pearson, etc. The cardinality k demonstrates the complication of the nearest-neighbor model; less adaptive models are achieved by higher values of K.

The output of decision making module will result in maintenance personnel's taking the "right" maintenance actions. The provided information should detect bearing faulty state as well as a precise fault identification.

4. Results and discussion

Three classes have been defined for the classifier: bearing healthy condition, ball fault and outer race way fault. Forty-eight vibration and load signals in various conditions of fault severity, load level and rotating speed have been fed into our automatic condition-based monitoring system during the training phase. The classifier uses these training data to provide the decision boundaries for each sensor, as shown in Figs. 7 and 8. Each point is resulted from applying principal component analysis to a feature matrix of which rows are feature vectors. As it was mentioned earlier, each of the feature vectors consists of 12 signal features. Some part of feature matrix of vibration and load signals are respectively demonstrated in Tables 1 and 2.

In this study, a logical method was used according to the specifications of each sensor. The training results demonstrate that the load cell is powerful to detect the healthy ball bearings from the defected ones. As can be seen in Fig. 7, the results of healthy bearings are completely distinct from the results of defected bearings, whereas the accelerometer is useful to detect the location of the fault. As can be seen in Fig. 8, accelerometer is so effective to detect the position of the faults. It is obvious in Fig. 8 that the accelerometer is inaccurate in recognition of the healthy bearing from the bearings with small outer race defects.

Finally, six signals of acceleration and six signals of load cell are used to examine the performance of the proposed system. The test data are assigned by the trained classifier to one particular classes under consideration based on the measured features.

Table 3 summarizes the actual bearing conditions and the defect classes which assign to each bearing by accelerometer, load cell and data fusion. As seen in Table 3, condition monitoring by only accelerometer gives one false answer. It is apparent that vibration measurement is very effective technique to detect the type of bearing defect. Mean while, condition monitoring by load cell is very sensitive to detect healthy bearings from defective bearings. However, the fusion of data from two sensors provides the best performance in detection.

However, this is a very good result considering that the extractor module only feeds two features into the classifier, for each signal entered the signal processing unit. Such system helps having a visual representation of classification process.

All results of the three cases prove that the fusion of data from different sensors provide more information than the data from single ones. In fact, the multi-sensor fusion technique improves accuracy and robustness in fault detection of bearing.

5. Conclusion

Multiple different sensors mounted on bearings provide information that would not be available from the single sensors. The fusion of data from different sensors enhances fault detection and diagnosis by supplying complementary information.

In this paper, a CBM system was proposed to predict and detect bearing failure by two sensors; accelerometer and load cell. In this CBM system, the waterfall fusion model was adopted as the fusion technique to optimally combine sensor data and achieve the hest decisions on the overall health of bearing components. The proposed method was applied to three cases of bearing fault detection and its results were compared with the results of conventional methods using individual sensors. In conclusion, the experimental results show the benefits of the proposed method for improving fault detection and diagnosis accuracy.

References

[1] N. Tandon, A. Choudhury, A review of vibration and acoustic measurement methods for the detection of defects in rolling element bearings, Tribology International 32 (1999) 469–480.
[2] J. Seo, H. Yoon, H. Ha, D. Hong, W. Kim, Infrared thermographic diagnosis mechanism for fault detection of ball bearing under dynamic loading conditions, Advanced Materials Research 295–297 (2011) 1544–1547.
[3] A. Zmitrowicz, Wear debris: a review of properties and constitutive models, Journal of Theoretical and Applied Mechanics 43 (2005) 3–35.
[4] S.H. Ghafari, F. Golnaraghi, F. Ismail, Fault diagnosis based on chaotic vibration of rotor systems supported by ball bearings, Proceeding of COMADEM 2006 (2006) 819–826.
[5] A.M. Al-Ghamd, D. Mba, A comparative experimental study on the use of acoustic emission and vibration analysis for bearing defect identification and estimation of defect size, Mechanical Systems and Signal Processing 20 (2006) 1537–1571.
[6] S. Bagavathiappan, B.B. Lahiri, T. Saravanan, John Philip, T. Jayakumar, Infrared thermography for condition monitoring – a review, Infrared Physics & Technology 60 (2013) 33–55.
[7] O.G. Gustafsson, T. Tallian, Research report on study of the vibration characteristics of bearings, Report: AL631023, Reg. 585 14:422 3, (1963), SKF Inc.
[8] C.S. Sunnersjö, Varying compliance vibrations of rolling bearings, Sound and Vibration 58 (1978) 363–373.
[9] D. Logan, J. Mathew, Using the correlation dimension for vibration fault diagnosis of rolling element bearings – I, Basic concepts, Mechanical Systems and Signal Processing 10 (1996) 241–250.
[10] D. Logan, J. Mathew, Using the correlation dimension for vibration fault diagnosis of rolling element bearings – II. Selection of experimental parameters, Mechanical Systems and Signal Processing 10 (1996) 251–264.
[11] F.K. Choy, J. Zhou, M.J. Braun, L. Wang, Vibration monitoring and damage quantification of faulty ball bearings, Journal of Tribology 127 (2005) 776–783.
[12] N. Tandon, A comparison of some vibration parameters for the condition monitoring of rolling element bearings, Measurement 12 (1994) 285–289.
[13] D.E. Butler, The shock pulse method for detection of damaged rolling bearings, NDT International 6 (1973) 92–95.
[14] J.I. Taylor, Identification of bearing defects by spectral analysis, Mechanical Design 102 (1980) 199–204.
[15] C.C. Osuagwu, D.W. Thomas, Effect of inter-modulation and quasi periodic instability in the diagnosis of rolling element incipient defect, Mechanical Design 104 (1982) 296–302.
[16] D. Ho, R.B. Randall, Optimization of bearing diagnostic techniques using simulated and actual bearing fault signals, Mechanical Systems and Signal Processing 14 (2000) 763–788.
[17] F. Bolaers, O. Cousinard, P. Marconnet, L. Rasolofondraibe, Advanced detection of rolling bearing spalling from de-noising vibratory signals, Control Engineering Practice 12 (2004) 181–190.
[18] M.S. Safizadeh, A.A. Lakis, M. Thomas, Time-frequency algorithms and their applications, International Journal of Computers and their Applications 7 (2000) 167–186.
[19] S. Prabhakar, A.R. Mohanty, A.S. Sekhar, Application of discrete wavelet transform for detection of ball bearing race fault, Tribology International 35 (2002) 793–800.
[20] C.J. Li, J. Ma, Wavelet decomposition of vibrations for detection of bearing localized defects, NDT&E International 30 (1997) 143–149.
[21] N.G. Nikolaou, I.A. Antoniadis, Rolling element bearing fault diagnosis using wavelet packets, NDT&E International 35 (2002) 197–205.
[22] B. Samanta, K.R. Al-Balushi, Artificial neural network based fault diagnostics of rolling element bearings using time domain features, Mechanical Systems and Signal Processing 17 (2003) 317–328.
[23] L.B. Jack, A.K. Nandi, A.C. McCormick, Diagnosis of rolling element bearing faults using radial basis function networks, Applied Signal Processing 6 (1999) 25–32.
[24] G. Vachtsevanos, P. Wang, Fault prognosis using dynamic wavelet neural networks, IEEE Systems Readiness Technology (2001) 857–870.
[25] S.H. Ghafari, F. Golnaraghi, F. Ismail, Rolling element bearings fault diagnosis based on neuro-fuzzy inference system, In: Proceeding of CMVA 2006, Canadian Machinery Vibration Association, 2006.
[26] X.Z. Shi, H. Chen, R.Q. Liu, H.Q. Sun, A PC-based fault diagnostic and quality evaluation system for ball bearing, In: Proceeding of 2nd international Machinery Monitoring and Diagnostics conference, COMADEM 90, (1990) 259–263.
[27] J.K. Spoerre, Application of the cascade correlation algorithm (CAA) to bearing fault classification problems, Computers in Industry 32 (1997) 295–304.
[28] T.I. Liu, J.H. Singonahalli, N.R. Iyer, Detection of roller bearing defects using expert system and fuzzy logic, Mechanical Systems and Signal Processing 10 (1996) 595–614.
[29] J. Yang, Y. Zhang, Y. Zhu, Intelligent fault diagnosis of rolling element bearing based on SVMs and fractal dimension, Mechanical Systems and Signal Processing 21 (2007) 2012–2024.
[30] B. Samanta, K.R. Al-Balushi, S.A. Al-Araimi, Bearing fault detection using artificial neural networks and genetic algorithm, EURASIP, Applied Signal Processing (2004) 366–377.
[31] A. Malhi, R.X. Gao, Recurrent neural networks for long-term prediction in machine condition monitoring, Instrumentation and Measurement Technology Conference (2004). 2048-20.
[32] N. Gebraeel, M. Lawley, R. Liu, V. Parmeshwaran, Residual life prediction from vibration based degradation signals: a neural network approach, IEEE Transactions on Industrial Electronics 51 (2004) 694–700.
[33] R. Huang, L. Xi, X. Li, C.R. Liu, H. Qiu, J. Lee, Residual life prediction for ball bearings based on self-organizing map and back propagation neural network methods, Mechanical Systems and Signal Processing 21 (2007) 193–207.
[34] T. Ingarashi, B. Noda, E. Matsushima, A study on the prediction of abnormalities in rolling bearing, JSLE 1 (1980) 71–76.